4.5 A WRF-DART study of the nontornadic and tornadic supercells intercepted by VORTEX2 on 10 June 2010

ALICIA M. KLEES * AND YVETTE P. RICHARDSON

The Pennsylvania State University, University Park, Pennsylvania.

GLEN ROMINE

National Center for Atmospheric Research, Boulder, Colorado

1. Introduction

On 10 June 2010, the second Verification of the Origins of Rotation in Tornadoes Experiment (VORTEX2) intercepted a nontornadic and tornadic supercell evolving in proximity to each other near Last Chance, Colorado. An analysis of mobile mesonet, mobile radar, 88D radar, StickNet, and mobile sounding data was completed to investigate why one supercell produced no tornadoes and the other, two (Klees et al. 2016). This observational study suggested that a combination of differing impacts of a storm merger on both supercells and an evolving storm environment likely played a significant role.

A new cell ('Cell A') developed between the two supercells and merged with both (Fig. 1). Cell A's merger with the nontornadic supercell led to the demise of this supercell, as evidenced by the decrease in dual-Doppler derived updraft and mesocyclone strength as the merger progressed (Klees et al. 2016). On the other hand, the mergers of Cell A and another new cell, 'Cell B,' with the tornadic supercell (Fig. 1) had seemingly no adverse impacts on the storm, as the tornadic supercell subsequently produced two tornadoes.

Additionally, 0–1 km storm-relative helicity (SRH1) was higher in the environment of the tornadic supercell (150 and 241 $m^2\ s^{-2}$) than in the environment of the nontornadic supercell (44 and 166 $m^2\ s^{-2}$) (Klees et al. 2016). The storm environment, in terms of SRH1, became more favorable for tornado production over time; from 2354 UTC to 0042 UTC in particular, SRH1 values tripled and 0–3 km storm-relative helicity (SRH3) values increased as well (Klees et al. 2016) (Fig. 2).

Given that the nontornadic supercell died 'prematurely,' perhaps this storm simply did not have the opportunity to experience this enhanced environment the way the tornadic supercell did? Perhaps the nontornadic supercell, had it not experienced the merger, would have otherwise produced tornadoes? Did the mergers of Cells A and B with the tornadic supercell make tornado production more likely than it otherwise would have been?

Such questions can only be fully investigated in a modeling study, especially given the lack of observations during the mergers and tornado production. In this study, the WRF-DART modeling framework will be used to examine the following:

1. Impacts of the evolving storm environment on tornado production
2. Potential for tornado production in the nontornadic supercell had the merger not occurred
3. Impacts of the merger on the tornadic supercell's tornado production (e.g., favorable modification of baroclinicity and/or convergence)
4. How the merger killed the nontornadic supercell

Thus far, the first point is under investigation.

2. Methods

Real-data simulations were completed for the 10 June 2010 case using the Weather Research and Forecasting Model v. 3.8 (WRF; Skamarock et al. 2008) and the Data Assimilation Research Testbed (DART; Anderson et al. 2009) framework. WRF simulations were run on a 3-km grid, with 51 vertical levels. Physics schemes used include YSU (boundary layer), Morrison (microphysics), RRTM (longwave radiation), Dudhia (shortwave radiation), revised MM5 (surface layer), and NOAH (land surface). An ensemble of 50 members (e.g., Romine et al. 2013) was initialized 12 hours prior to storm initiation on 10

Corresponding author address: Alicia M. Klees, Department of Meteorology, The Pennsylvania State University, 503 Walker Building, University Park, PA 16802.
E-mail: amk5375@psu.edu

June (Fig. 3). To generate this ensemble, random perturbations from WRFDA-3DVAR, CV3 option (Torn and Hakim 2008) were added to fields from the 0.5° GFS (6 UTC) forecast. To create a more realistic mesoscale environment (e.g., Romine et al. 2013; Jones et al. 2015), conventional observations were assimilated hourly onto the grid (Fig. 4) using the Ensemble Adjustment Kalman Filter in DART (Anderson 2001). These observations, acquired from the Global Systems Division (GSD) Meteorological Assimilation Data Ingest System (MADIS), include rawinsonde (u, v, T, q, altimeter), standard aviation routine weather reports (METAR) (u, v, T, T_d, altimeter), Aircraft Meteorological Data Relay (ADMAR) reports (u, v, T, T_d), and wind profiler (u, v).

3. Results

Preliminary results suggest promise in the ability of WRF-DART to reproduce the storm environment on 10 June. For example, simulations using only WRF do not well capture the tongue of moisture in northeastern CO at 22 UTC (a bit prior to the initiation of the storms) (Fig. 5a,c); the simulated environment has dewpoints in the upper 20s °F in the initiation region. However, with the assimilation of conventional observations, the environment is much moister and closer to reality, with dewpoints now in the upper 40s–low 50s °F (Fig. 5b,c). Preliminary evaluation of patterns in simulated SRH1 (not shown) shows promise.

The simulations thus far do not well reproduce the two supercells, even with the assimilation of conventional observations (Fig. 6). Although the general timing and location of the convection is fairly realistic, the convection produced is very weak and unstructured and not of a discrete supercellular mode. The assimilation of radar data (see 'Future work' for details) should significantly help WRF generate the 10 June supercells.

4. Summary and conclusions

On 10 June 2010, VORTEX2 intercepted a tornadic and a nontornadic supercell evolving in proximity to each other. An observational study suggested that a combination of an evolving storm environment and differing impacts from storm merger(s) may have led to the difference in tornado production on this day. The storm environment became more supportive of tornado production over time, especially in terms of SRH1. The merger with Cell A led to the demise of the nontornadic supercell, but the merger of Cells A and B with the tornadic supercell potentially could have helped this supercell produce tornadoes. A promising WRF-DART study is underway to investigate the role of the merger(s) and storm environments on the supercells and tornado production on 10 June.

5. Future work

Future work includes using a boundary layer scheme that mixes less aggressively than YSU (e.g., MYJ), to more appropriately handle the sometimes shallow moist layers in Colorado. Other future work involves the assimilation of further observations (especially radar), to realistically produce the two supercells and mergers so the role of the mergers on this day can be investigated. Around 2 hours prior to storm initiation, a 600-m grid will be nested within the 3-km grid to resolve important storm-scale processes (Fig. 3). Data from the Denver WSR-88D radar (radial velocity, reflectivity, and clear-air reflectivity) will be assimilated onto the 600-m grid (Fig. 3) every 15–30 minutes prior to the initiation of the storms and during the early stages of evolution, and at a higher frequency (every 2 minutes; e.g., Marquis et al. 2014, 2016) closer to the time of the storm mergers. VORTEX2 observations from three mobile radars (radial velocity and clear-air reflectivity) will also be assimilated onto this grid every 2 minutes. VORTEX2 observations from mobile mesonet and mobile soundings will be assimilated as well (Fig. 3).

Acknowledgments. We are grateful to Paul Markowski, Jim Marquis, David Stensrud, Jeff Anderson, Terra Ladwig, Curtis Alexander, David Dowell and the mesoscale research group at Penn State University for helpful discussions. We also thank all VORTEX2 PIs and participants for the comprehensive data collection on 10 June. Conventional observation data access was provided by MADIS. This research would not have been possible without high-performance computing support from Yellowstone (ark:/85065/d7wd3xhc) provided by NCAR's Computational and Information Systems Laboratory, sponsored by the National Science Foundation. Klees and Richardson were supported by NSF-AGS-1157646 and NSF-AGS-1536460.

References

Anderson, J., 2001: An ensemble adjustment Kalman filter for data assimilation. *Mon. Wea. Rev.*, **129**, 2884–2903.

Anderson, J., T. Hoar, K. Raeder, H. Liu, N. Collins, R. Torn, and A. Avellan, 2009: The Data Assimilation Research Testbed: A community facility. *Bull. Amer. Meteor. Soc.*, **90**, 1283–1296.

Jones, T., D. Stensrud, L. Wicker, P. Minnis, and R. Palikonda, 2015: Simultaneous radar and satellite data storm-scale assimilation using an ensemble Kalman filter approach for 24 May 2011. *Mon. Wea. Rev.*, **143**, 165–194.

Klees, A., Y. Richardson, P. Markowski, C. Weiss, J. M. Wurman, and K. K. Kosiba, 2016: Comparison of the tornadic and nontornadic supercells intercepted by VORTEX2 on 10 June 2010. *Mon. Wea. Rev.*, **144**, 3201–3231.

Marquis, J., Y. Richardson, P. Markowski, D. Dowell, J. Wurman, K. Kosiba, P. Robinson, and G. Romine, 2014: An investigation of the Goshen County, Wyoming, tornadic supercell of 5 June 2009 using EnKF assimilation of mobile mesonet and radar observations collected during VORTEX2. Part I: Experiment design and verification of the EnKF analyses. *Mon. Wea. Rev.*, **142**, 530–554.

Marquis, J., Y. Richardson, P. Markowski, J. Wurman, K. Kosiba, and P. Robinson, 2016: An investigation of the Goshen County, Wyoming, tornadic supercell of 5 June 2009 using EnKF assimilation of mobile mesonet and radar observations collected during VORTEX2. Part II: mesocyclone-scale processes affecting tornado formation, maintenance, and decay. *Mon. Wea. Rev.*, **144**, 3441–3463.

Romine, G., C. Schwartz, C. Snyder, J. Anderson, and M. L. Weisman, 2013: Model bias in a continuously cycled assimilation system and its influence on convection-permitting forecasts. *Mon. Wea. Rev.*, **141**, 1263–1284.

Skamarock, W., and Coauthors, 2008: A description of the Advanced Research WRF version 3. NCAR Tech. Note NCAR/TN-475+STR. , 113 pp.

Torn, R., and G. Hakim, 2008: Performance characteristics of a pseudo-operational ensemble Kalman filter. *Mon. Wea. Rev.*, **136**, 3947–3963.

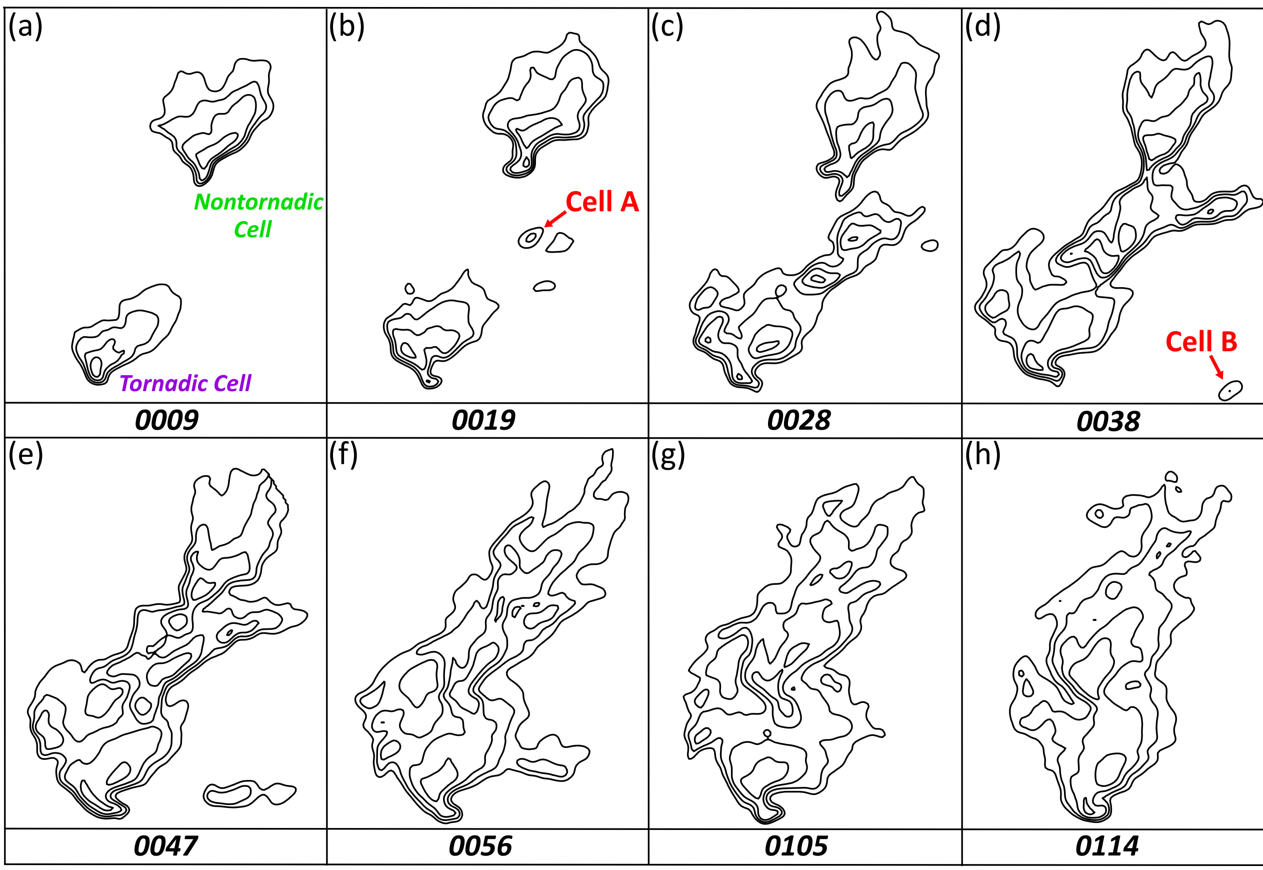

FIG. 1. From Klees et al. (2016). Interactions between Cells A and B (denoted in red) and the original supercells over time. Contours are of KFTG-88D logarithmic equivalent reflectivity factor, beginning at 25 dBZ for every 10 dBZ (0009–0047 UTC at 1.5 km and 0056–0114 UTC at 2 km).

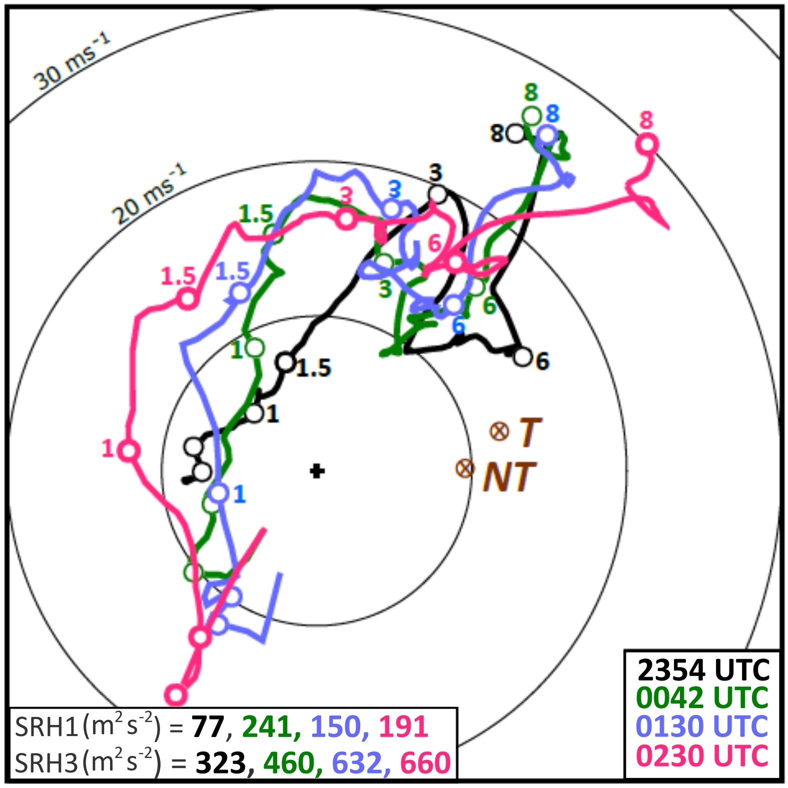

FIG. 2. Adapted from Klees et al. (2016). Temporal evolution of the hodographs from 2354–0230 UTC from the NCAR1 2354 (black), NCAR1 0042 (green), NSSL1 0130 (blue), and NSSL1 0230 (pink) soundings (which were collected at similar locations). Numbers along the hodograph are heights (km AGL). The two unlabeled circles denote heights of 250 and 500 m. Labeled brown cross-hatched circles denote the storm motion of the tornadic and nontornadic supercells. The chart shows values of SRH1 and SRH3 (calculated using storm motion from the tornadic supercell) for the hodographs.

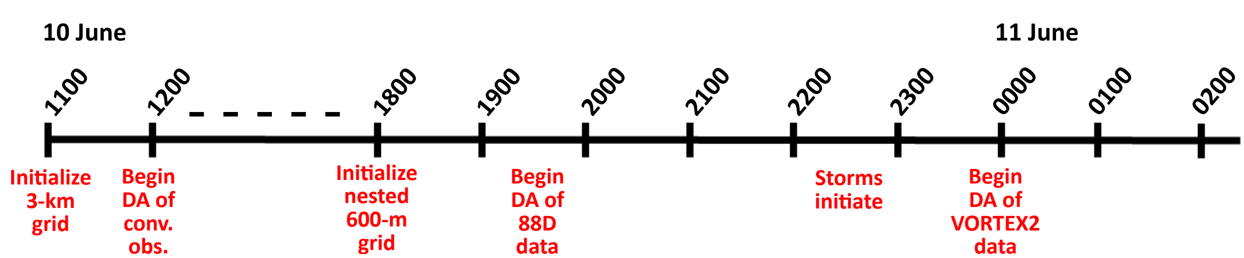

FIG. 3. Timeline of the WRF-DART simulations. Times are in UTC.

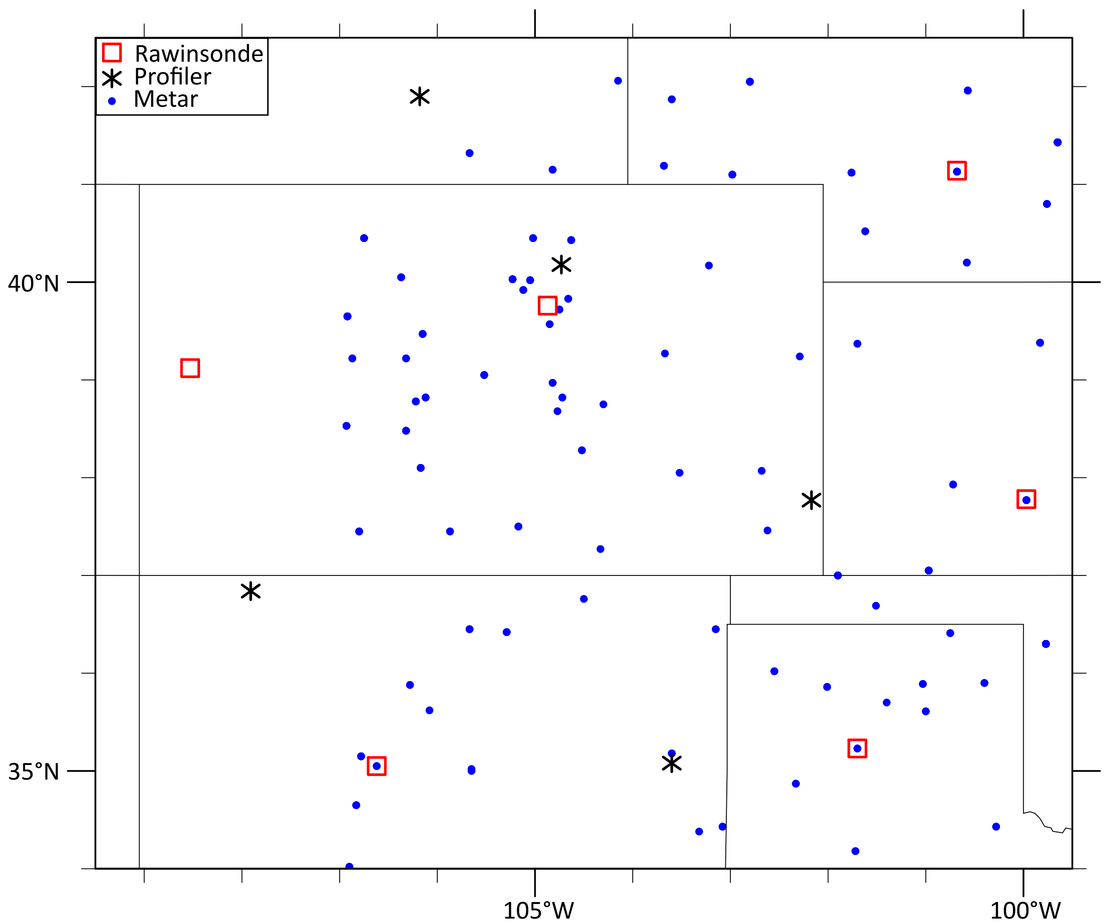

FIG. 4. Location of conventional observations (rawinsonde, red square; profiler, black asterisk; metar, blue dot) available to be assimilated onto the 3-km domain at 12 UTC. Aircraft observations are not plotted for the sake of clarity.

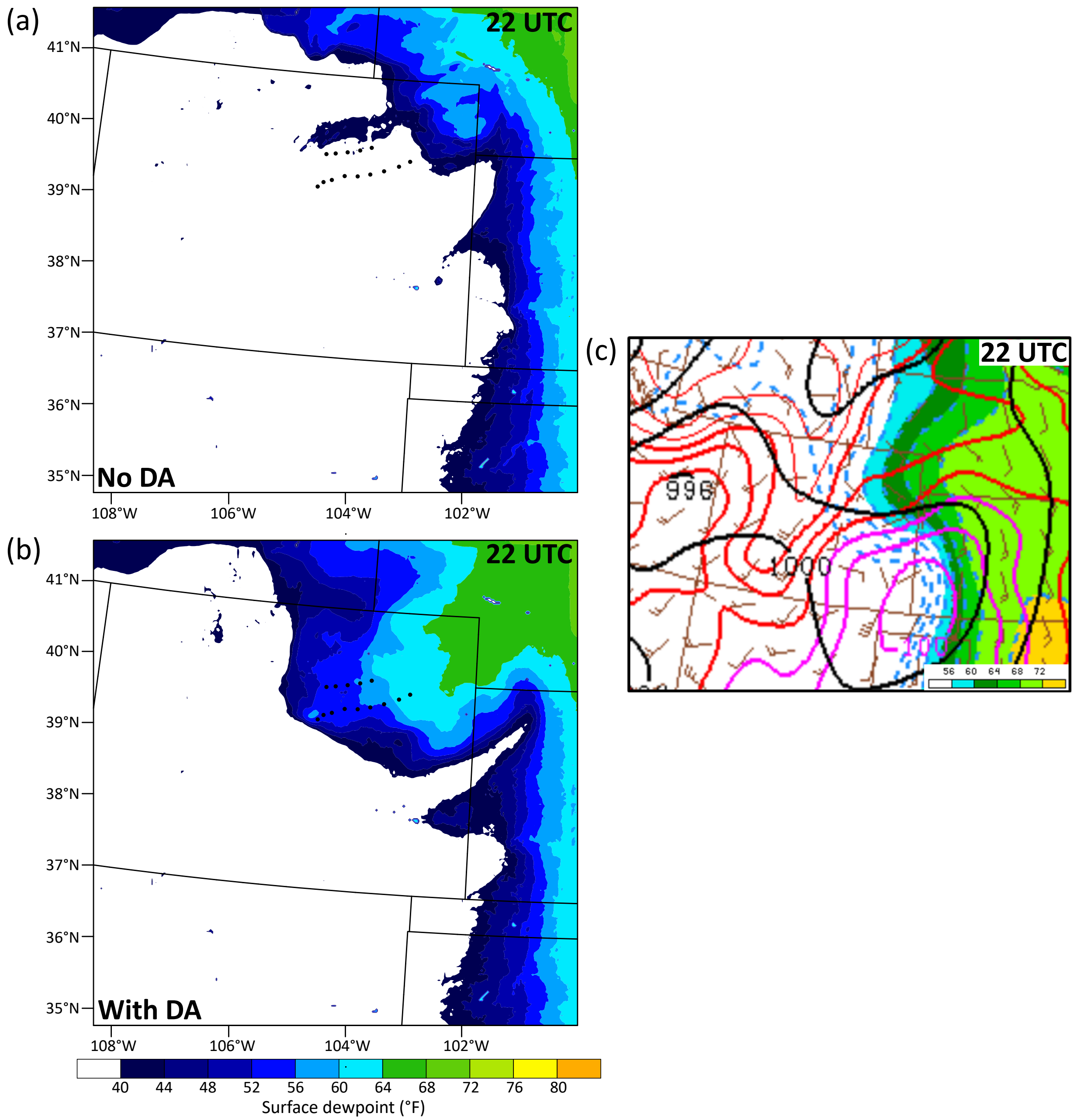

FIG. 5. Modeled surface dewpoints (°F) at 22 UTC from 3-km WRF simulations with (a) no data assimilation and (b) assimilation of conventional observations (ensemble mean shown here). The northern and southern dot tracks are the actual paths of the nontornadic and tornadic supercells, respectively. (c) Actual dewpoints at 22 UTC (from the SPC mesoanalysis).

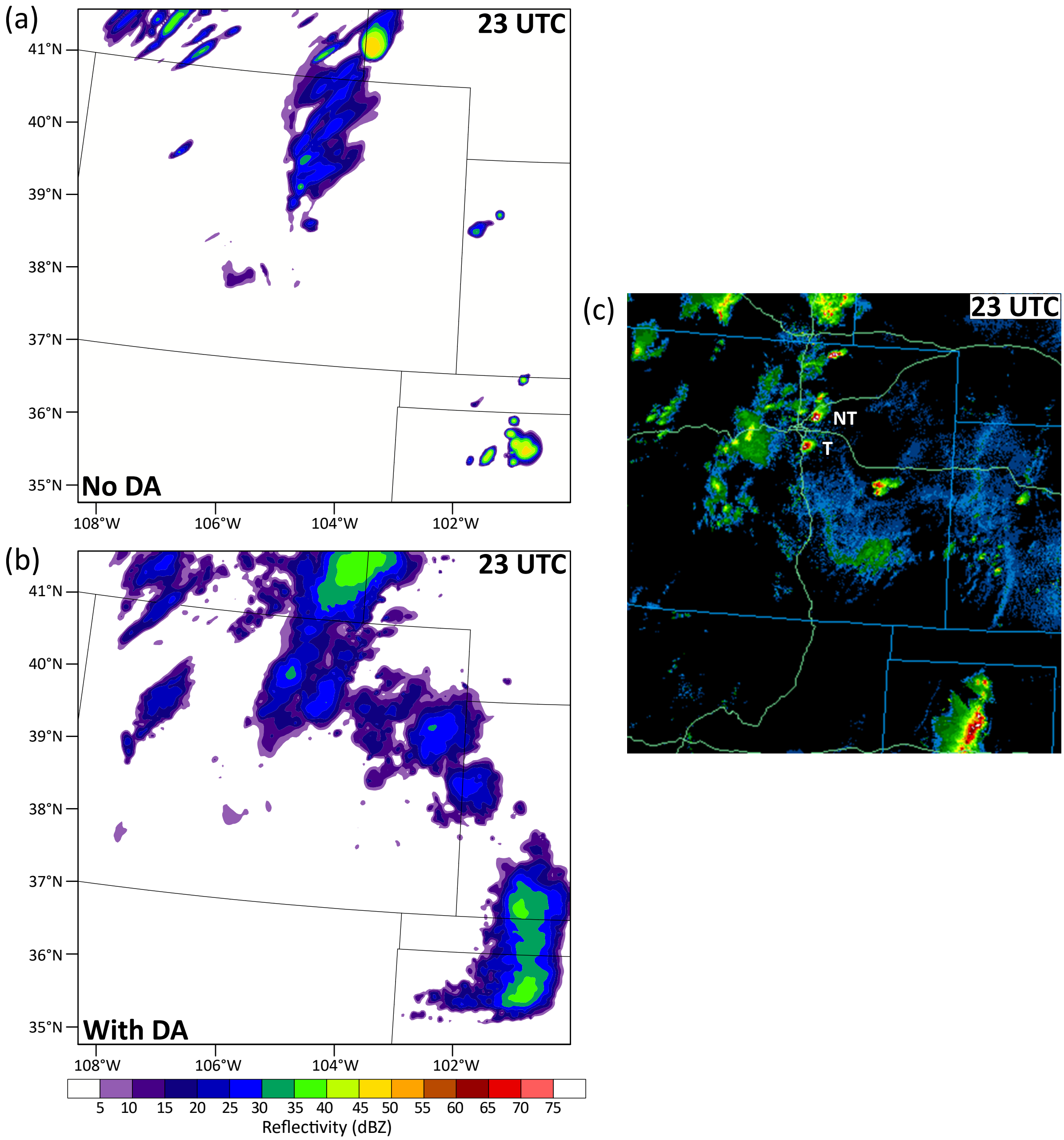

FIG. 6. Modeled reflectivity (dBZ) at 23 UTC from 3-km WRF simulations with (a) no data assimilation and (b) assimilation of conventional observations (ensemble mean shown here). (c) Actual reflectivity at 23 UTC, with the nontornadic and tornadic supercells denoted.